# INTERACTION OF A CONICAL SHOCK WAVE WITH A TURBULENT BOUNDARY LAYER

ICAS-92-4.8.2

S. L. Teh and S. L. Gai
Department of Mechanical Engineering, University College, U.N.S.W.,
Australian Defence Force Academy, Canberra, Australia.

## Abstract

The paper reports an investigation on the interaction of an incident conical shock wave with a turbulent boundary layer. Although a conical shock theoretically creates a hyperbolic shock trace on the flat plate, the line joining all the experimental interaction origins takes a different form due to varying upstream influence. The existence of strong pressure gradients in the spanwise direction after the shock leads to the boundary layer twist. A model based on the upstream influence of the shock when combined with McCabe's Secondary Flow Theory showed separation to occur at an external flow deflection of 11.8°. The oil flow measurements however show this to occur at 9.2°. This discrepancy is of the same order as that found by McCabe. Detailed data involving Schlieren and shadowgraph photography, surface flow visualization and surface pressure measurements are presented.

## Notation

Symbols

| | |
|---|---|
| a,b | parameters of hyperbola |
| L | upstream influence |
| M | Mach number |
| p | static pressure at wall |
| Re | Reynolds number |
| S | singular point |
| x, y, z | system of Cartesian coordinates |
| $\beta$ | shock wave angle |
| $\Delta$ | external flow deflection through shock |
| $\varepsilon$ | extra deflection of surface streamlines |
| $\psi$ | angle of yaw |
| $\theta$ | external flow deflection through shock |
| $\rho$ | density |
| $\gamma$ | specific heat ratio |
| $\zeta$ | inclination of shock wave to undisturbed stream in McCabe's model (Fig. 13) |

Subscripts

| | |
|---|---|
| s | new "shock front" |
| u | streamwise extent |
| y | spanwise direction |
| 1 | upstream of shock wave |
| 2 | downstream of shock wave |
| 12 | across oncoming shock |
| $\infty$ | freestream conditions |
| max | maximum |



## I. Introduction

Some understanding of the 3-D shock/boundary layer interaction has been achieved in recent years but, these studies have generally been confined to what is known as 'glancing or swept shock interactions'[1,2]. An interesting 3-D problem is that of interaction between an incident conical shock and a 2-D boundary layer on a plane surface. This problem has practical relevance, for example, in side intakes with centre bodies of supersonic aircraft and ramjets. A literature review has shown that only Migotsky and Morkovin's[3] inviscid analysis of reflection of a conical shock from a plane surface and Panov's experimental study[4] of conical shock /2-D boundary layer interaction, exist in the open literature. A related problem, that of an incident conical shock interacting with a turbulent boundary layer on a cylindrical surface has recently been studied[5].

This paper presents the flow model, the experimental data and their correlations for the interaction of an incident conical shock wave with a plane turbulent boundary layer.

## II Experimental Arrangement

The experiments were carried out in a blow down supersonic wind tunnel of cross section 155 mm x 90 mm at a Mach number M = 2.0 and freestream unit Reynolds number of 30 x $10^6$ $m^{-1}$ and 58 x $10^6$ $m^{-1}$.

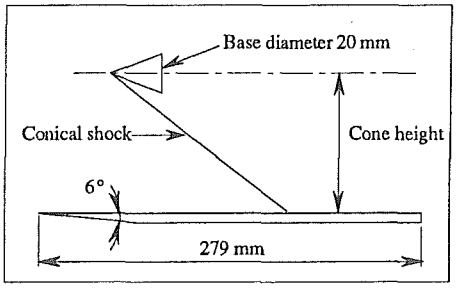


Fig.1 Experimental Arrangement

The models were half-cones with cone angles ranging from 14° to 40° and full-cones with cone angles of 28°, 40° and 60°. The cone base diameter was 20 mm. The flat plate was 269 mm long, 150 mm wide and 9 mm thick with a 6° leading edge [see Figure 1]. The two-dimensional boundary layer thickness on the plate varied between 2.2 mm to 2.4 mm in the region of interaction.

The techniques employed for acquisition of data consisted of Schlieren and shadowgraph photography, surface flow visualization and surface pressure measurements.

Preliminary investigations using flow visualization techniques were carried out with 20°, 30° and 40° half-cones mounted at heights of 30 mm, 45 mm and 60 mm. The half-cones were positioned in the stream-wise direction in such away that the shocks generated interacted with the flat plate boundary layer at the same location knowing the shock wave angles from established charts[6]. Full investigations were then carried out with half-cones of angles ranging from 14° to 26° and full-cone of 28°, 40° and 60° all mounted at height of 30 mm above the flat plate.

## III Oil-Flow Patterns

### IIIa. Three Dimensional Separation

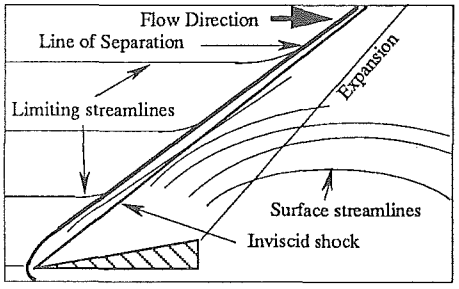


Fig. 2 Separated Boundary Layer Oil Flow Pattern (Ref. 1)

McCabe[1] studied swept shock wave/boundary layer interaction with a sharp unswept fin. He adopted Maskell's separation criterion which is that separation line must be an envelope of the limiting streamlines upstream of the shock as shown in Figure 2. This figure reproduced from McCabe[1] is a schematic representation of the oil flow patterns, showing separated boundary layer on the side wall at a Mach number of 1.96 when a wedge in a plane perpendicular to the wall was used to create the shock. The oil filaments do not break away from the wall at separation, but instead turn approximately parallel to the shock and run together to form an envelope along the separation line.

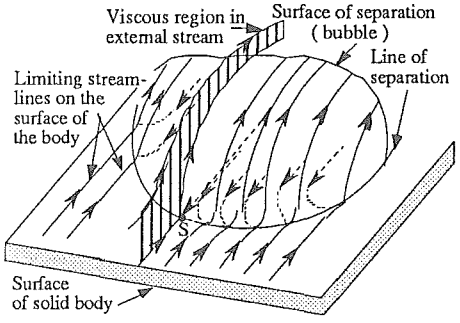


Fig. 3 Separation in Three Dimensions

In Maskell's[7] model of three-dimensional separation, two basic components are free shear (or vortex) layers and bubbles as shown in Figure 3. The surface of separation encloses fluid which is not part of the main stream but is carried along with the body. The bubble formation requires the existence of one singular point S, where the behaviour of the flow is the same as near a separation point in two-dimensional flow. The limiting streamlines on the surface of the solid body join the line of separation tangentially.

### IIIb. Conical Shock/Boundary Layer Interaction

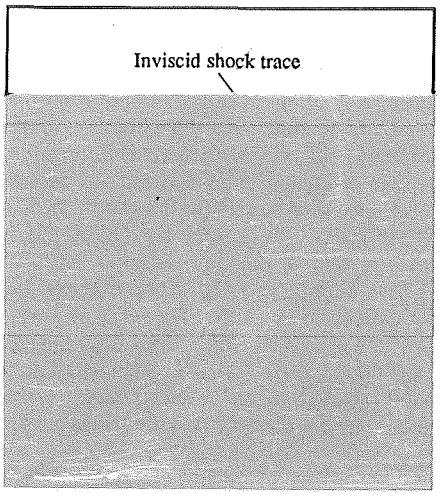


Fig. 4 Oil Flow Pattern, 14° Half-Cone.

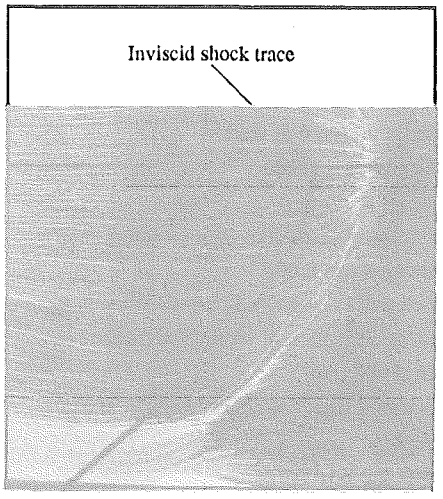


Fig. 5 Oil Flow Pattern, 17° Half-Cone.

Figure 4 shows oil-flow patterns obtained on the flat plate at a Mach number of 2.0 when a 14° half-cone mounted at a height of 30 mm was used to generate the conical shock. The inviscid shock has been overlaid on the photograph to indicate its location. The deflections of the surface streamlines are sudden in the vicinity of the line of symmetry and they tend to be gradual away from it. There is no deflection at the line of symmetry. Away from the line of symmetry, the deflection initially increases to a maximum and then decreases.

Similarly, Figure 5 shows oil-flow patterns obtained on the flat plate with a 17° half-cone. All the surface streamlines

after the shock originate from the the vertex of the shock trace. The boundary layer has separated as indicated by the upstream limiting surface streamlines running parallel to the shock to form an envelope along the separation line.

Figure 6 shows oil-flow patterns obtained on the flat plate with a 24° half-cone mounted at the same height as before. With the increased shock strength, the line of separation shifts further upstream. Surface streamlines originating from the line of reattachment travel in both upstream and downstream directions. Reverse flow occurs between the separation line and the reattachment line.

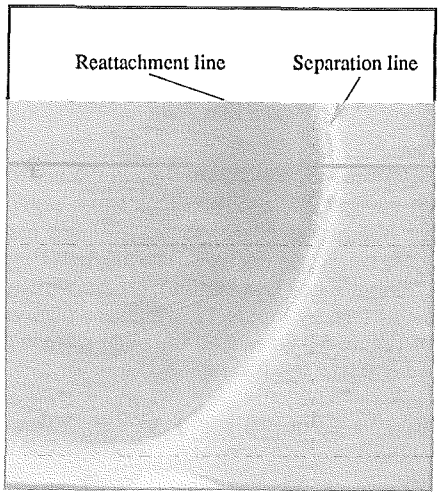


Fig. 6 Oil Flow Pattern, 24° Half-Cone.

Panov proposed a model for the incident conical shock/turbulent boundary layer interaction as shown in Figure 7[4]. The conical shock 1 and the three-dimensional shock 2 cause separation of boundary layer. The approaching flow passes through shock 2 and is deflected upward from the plate surface, then passes through shock 3, which is reflected from the upper jet boundary of the stagnant zone in the form of the rarefaction wave. After the rarefaction wave the flow velocity at the edge of the separated boundary layer is directed at some angle to the plate surface. The compression shock 7 turns the outer flow again parallel to the plate surface. The boundary layer, which has separated along line S, reattaches to the surface along the line e; this phenomenon and the flow in the separation zone 5 have a three-dimensional nature. Under certain conditions the rarefaction wave 6, which emanates from the trailing edge of the cone, affects the flow in the interaction region.

Because of the existence of lateral pressure gradients there is outflow of fluid from the plane of symmetry. A horseshoe vortex is observed in the reverse flow zone with its ends extending downstream on both sides of the line of symmetry. The vortex expands gradually as it enters the region with lower pressure, and the vortex flow breaks down. The boundary layer separation was observed only along the central portion of the line s. The ends of the line s are simply the trace of the interaction of the three-dimensional shock 2 with the boundary layer. In these regions the intensity of shock 2 is not sufficient to cause boundary-layer separation.

Examination of Panov's model in terms of Maskell's definition of three-dimensional separation discussed earlier would suggest that the surface of separation would contract from the line of symmetry and would eventually vanish. Flow direction of the external streamlines would act to inhibit reverse flow, eventually turning the flow around far away from the line of symmetry where the shock strength is the lowest.

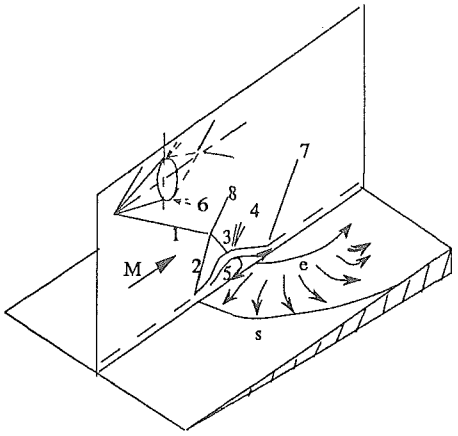


Fig. 7 Panov's Model for Conical Shock/2-D Boundary Layer Interaction

## IV. Development of Flow Model

### IVa. Conical Shock Incident on Flat Plate - Inviscid Case

Before considering the interaction of an incident conical shock and a planar boundary layer, let us consider the inviscid equations for the hyperbolic shock trace generated by an incident conical shock on a flat plate

The general equation of a hyperbola is

$$\frac{x^2}{a^2} - \frac{y^2}{b^2} = 1 \qquad (1)$$

Equation (1) is rearranged to express y as dependent variable

$$y = b\sqrt{\frac{x^2}{a^2} - 1} \qquad (2)$$

Figure 8 shows a hyperbola with its parameters a and b. The transverse axis is the segment AB of length 2a joining points (-a, 0) and (a, 0), while the conjugate axis is the segment CD of length 2b joining the points (0, -b) and (0,b). The parameter b is in fact the height at which the cone is mounted above the flat plate. This can be explained [Figure 9] by the fact the vertex of the conjugate of the hyperbola is a radial distance b from the apex of the cone.

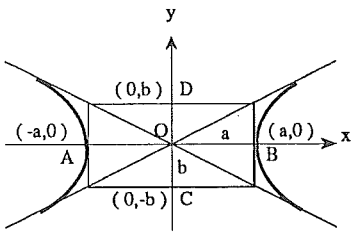


Fig. 8 Hyperbola

The parameter 'a' can also be expressed in terms of the shock wave angle $\beta_1$ and the height b as follows :

$$a = \frac{b}{\tan \beta_1} \qquad (3)$$

With known values of height b and shock wave angle $\beta_1$, and substituting Equation (3) into Equations (2), the hyperbolic shock trace due to the conical shock on the plain surface could be determined.

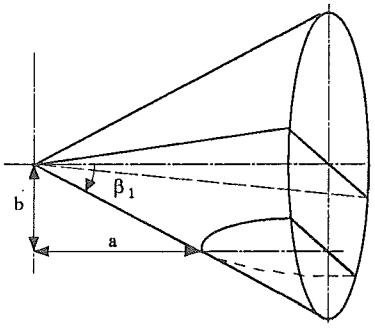


Fig. 9 Hyperbolic Shock Trace Generated by a Cone

The angle of yaw of the flow to any point of the hyperbola is also required for further analysis of the flow system. It is shown in Figure 10 as

$$\tan \psi = \frac{x}{y + \left( \frac{b^2}{y} \right)} \qquad (4)$$

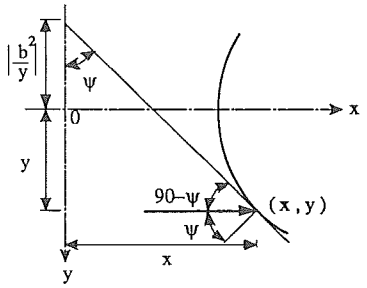


Fig. 10 Yaw Angle of the Flow

To obtain the deflection of the flow at the plate, the normal to every shock ray is firstly determined. This is the product of the initial upstream Mach number $M_1$ and the sine of the shock wave angle $\beta_1$. This product is termed here as the "normal Mach number". The shock wave angle $\beta_1$ between this ray and the free-stream remains constant following the shock trace out from the line of symmetry [see Figure 11].

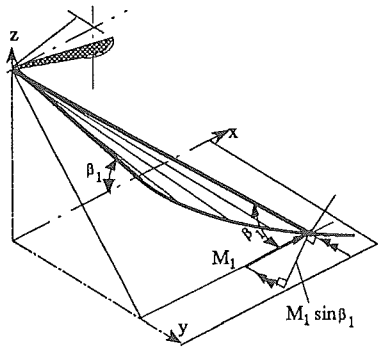


Fig. 11 Inviscid Conical Shock on a Flat Plate

To determine the deflection $\theta_{12y}$ in the y-direction, the initial Mach number $M_1$ and the shock wave angle $\beta_1$ in the equation for oblique shock wave angle[7] are respectively replaced by $M_1 \sin\beta_1$ and (90°-$\psi$). The angle (90°- $\psi$), termed here as the "lateral shock wave angle", is complimentary to the angle of yaw as seen by Figure 12, which is a plan view of the x-y plane of Figure 11 In fact, at the plate there is deflection only in the x-y plane and that is,

$$\tan \theta_{12y} = 2 \cot (90 - \psi) \times \frac{\left[ (M_1 \sin \beta_1)^2 \sin^2 (90°-\psi) - 1 \right]}{(M_1 \sin \beta_1)^2 \left[ \gamma + \cos (2(90°-\psi)) + 2 \right]} \qquad (5)$$

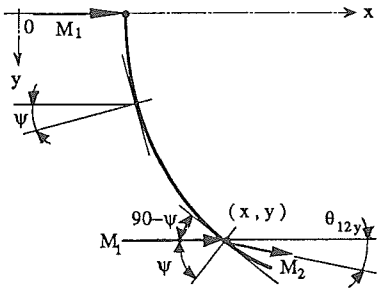


Fig.12 Deflection of Flow Through Inviscid Conical Shock

Similarly, the Mach number after the shock is

$$M_2^2 = \frac{1}{\sin^2 \left[ (90°-\psi) - \theta_{12y} \right]} \times \frac{1 + \frac{\gamma-1}{2} \left[ (M_1 \sin \beta)^2 \sin^2 (90°-\psi) \right]}{\gamma (M_1 \sin \beta)^2 \sin^2 (90°-\psi) - \frac{\gamma-1}{2}} \qquad (6)$$

Other corresponding relations across the shock such as pressure ratio and density ratio are,

$$\frac{p_2}{p_1} = 1 + \frac{2\gamma}{\gamma+1}[(M_1 \sin\beta)^2 \sin^2(90°-\psi)-1] \qquad (7)$$

$$\frac{\rho_2}{\rho_1} = \frac{(\gamma+1)(M_1 \sin\beta)^2 \sin^2(90°-\psi)}{(\gamma-1)(M_1 \sin\beta)^2 \sin^2(90°-\psi)+2} \qquad (8)$$

IVb. Conical Shock/Boundary Layer Interaction

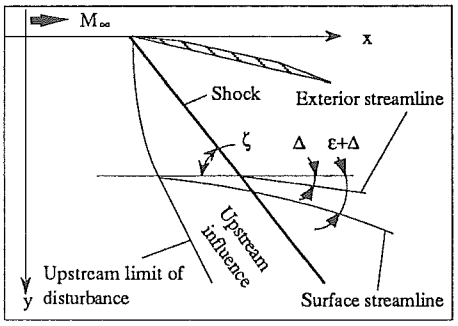


Fig. 13 Swept Shock/Boundary Layer Interaction (Ref. 1)

Before we consider the interaction of an incident conical shock with a boundary layer, we shall first examine the interaction of the shock wave generated by a sharp fin with a boundary layer. This interaction known as the swept shock/boundary layer interaction was first studied in detail by McCabe(1) and he proposed a model as shown in Figure 13.

In McCabe's model, the effects of pressure gradients caused by the shock are assumed to spread across the boundary layer which implies that deflections within the boundary layer are gradual unlike in the external flow. This means that since the normal pressure gradient is zero according to boundary layer approximation, the lateral pressure gradient will deflect the slower moving fluid near the surface through larger angles compared to the faster moving fluid fluid in the outer layers. Thus the boundary layer is skewed.

McCabe also describes this skewing in terms of the bending of the vortex tube axis in the boundary layer thus imparting a streamwise vorticity component that causes the streamlines in the boundary layer near the surface to deflect more than in the external stream producing secondary flow characteristics of three-dimensional boundary layers. However, it is assumed that vorticity is conserved during the process.

The separation criterion is when the inviscid shock wave angle $\zeta$ on the horizontal plane is less than or equal to the sum of the external flow deflection $\Delta$ through the shock and the extra deflection of the surface streamline $\varepsilon$ [see Figure 13]. The expression for the extra deflection of the surface streamline $\varepsilon$ is given by(1)

$$\tan\varepsilon = \frac{\sin(2\zeta - \Delta)\sin\Delta}{\cos^2\zeta \tan(\zeta - \Delta)} \qquad (9)$$

Let us now consider interaction region of the conical shock and the boundary layer. As a result of the boundary layer, an "interaction front" is formed due to positions defined by the varying upstream interaction lengths along the shock trace [see Figure 14]. The shape of the "interaction front" is determined by extrapolating to the wall the quasi-linear part of the surface pressure distribution(9).

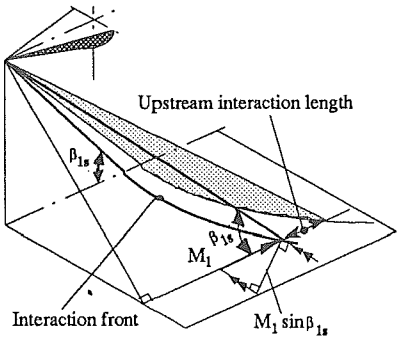


Fig.14 Conical Shock / Boundary Layer Interactions

New "shock rays" can be drawn for these positions. This leads to new "shock wave" angles and "yaw angles" for the flow. The new shock wave angle $\beta_{1s}$ is greater than the corresponding shock wave angle $\beta_1$ in the inviscid case. However, the shock wave angle $\beta_{1s}$ at any other location out from the vertex is no longer equal to the new shock wave angle at the line of symmetry. The strength of each ray is $M_1 \sin\beta_{1s}$.

It follows that the flow deflection which is denoted here as $\Delta_s$ instead of $\theta_{12y}$, across the "interaction front" in the y-direction of the exterior streamline can be determined by Equation (5). The extra deflection of the corresponding surface streamlines can then be found with Equation (9). We may term this scheme of determining the various flow parameters as the "virtual shock front" model.

Based on this, the flow field of an unseparated boundary layer will appear as shown in Figure 15.

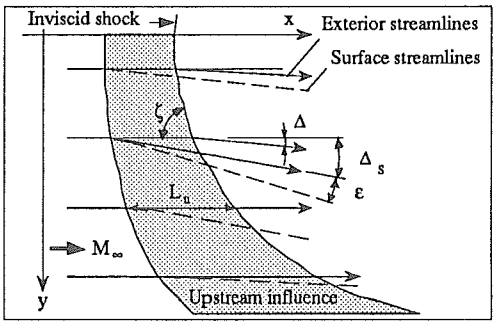


Fig. 15 Proposed Flow Field for Unseparated Boundary Layer

Outside the boundary layer, there is no lateral flow deflection at the line of symmetry. Away from the line of symmetry and just outside the boundary layer, the lateral deflection of the flow denoted here as $\Delta$, which is the same as $\theta_{12y}$ and is computed using Equation 5, initially increases to a maximum and then reduces to zero due to weakening of the shock. This lateral deflection of the external flow occurs

instantaneously. The corresponding shock wave angle is $\zeta$ and this is the same as the angle ($90°-\psi$) of Equation (5).

Similar to the swept shock/boundary layer interaction, deflection of the flow within the boundary layer is gradual due to spreading across the boundary layer effects of lateral pressure gradient caused by the shock. Therefore, the surface streamlines would be deflected through largest angles. The deflection of the surface streamlines originates at where the interaction starts. The surface streamlines would basically follow the lateral deflection pattern of the external flow but much more slowly.

As also observed in swept shock/boundary layer interaction, the region of upstream influence of the shock increases away from the line of symmetry despite the decreasing shock strength. This is shown by the increase in $L_u$ from the line of symmetry. This is a characteristic of three-dimensional interaction as remarked by Bogdonoff[9,11].

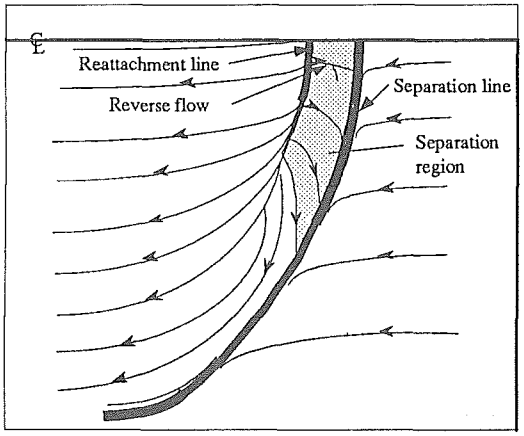


Fig. 16 Flow Field of Conical Flow with Separation.

A proposed flow field of separated boundary layer is shown in Figure 16. It basically resembles oil-flow patterns obtained on the flat plate with a 24° half-cone shown in Figure 6.

This figure shows how the area of the separation region decreases away from the line of symmetry. This is due to flattening out and eventual disappearance of the surface of separation at some distance away from the line of symmetry. It is then followed by a complete turn around of the flow in the boundary layer brought about by the opposite flow direction of the external streamlines.

## V. Pressure Measurements

Figure 17a shows the positions on the flat plate where the surface pressure data were gathered. The surface pressures for the seven data stations of the 14° half-cone are shown in Figure 17b. The initial rise in surface pressure varies with he streamwise position, being 158.9 mm from the leading edge at the line of symmetry A and 175.4 mm at Station G. The maximum surface pressure varies from 1.75 at Station A to 1.45 at Station F. As a result of sidewall effects, the maximum pressure at Station G is higher that that of Station F although it is a further 6 mm away from the line of symmetry.

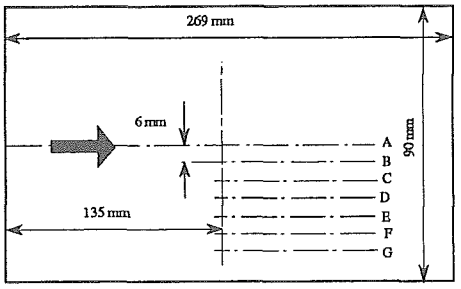


Fig. 17a Data Stations for Surface Pressure

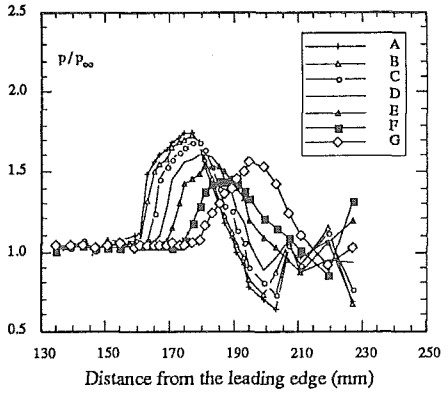


Fig.17b Surface Pressure Distribution, 14° Half-Cone at Re/m 58million

The surface pressure distribution for the 17° half-cone is shown in Figure 18. The boundary layer starts to separate with the shock generated by this half-cone. This was indicated by oil flow patterns in Figure 5 as discussed earlier. The respective maximum surface pressures at Station A and Station F are 1.98 and 1.48. These are higher than those of the 14° half-cone. Note that the pressure spread at all stations are smaller than those of the 14° half-cone.

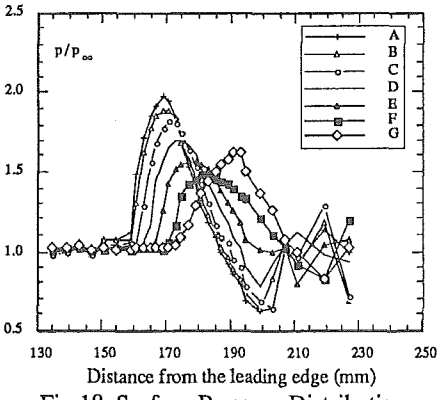


Fig.18 Surface Pressure Distribution, 17° Half-Cone at Re/m 58million

## VI. Further Discussion of Results

The "interaction front" and the inviscid shock trace for the 14° half-cone are shown in Figure 19a. The region of upstream influence increases away from the line of symmetry.

The external flow deflection $\Delta$ through the shock and the inclination of shock wave to undisturbed stream $\zeta$ are shown in Figure 19b. The external flow deflection through shock at the "interaction front" $\Delta_s$ , its corresponding extra deflection of the surface streamlines $\varepsilon$, and the total deflection of the streamlines ($\Delta_s+\varepsilon$) are also shown.

The calculated total deflection of the streamlines ($\Delta_s+\varepsilon$) follows closely that of the experimental surface streamlines $(\Delta+\varepsilon)_{oil}$ which is extracted from the oil flow photograph.

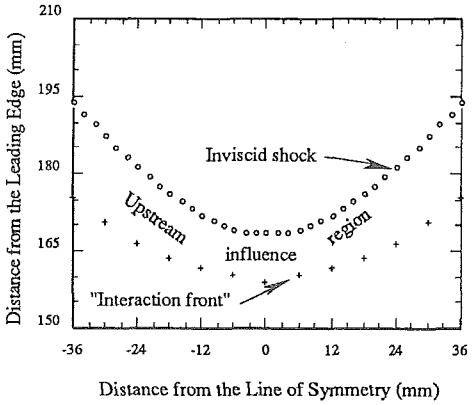


Fig. 19a Inviscid Shock Trace and Upstream Influence, 14°Half-Cone, Re/m 58 million

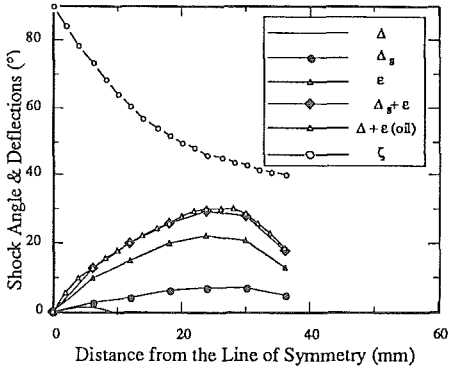


Fig.19b Lateral Shock Wave Angles and Deflections,14°Half-Cone, Re/m 58 million

Figure 20 shows for a 17° half-cone, all the flow angles as depicted in Figure 19b except the curve for the surface streamlines from oil flow which could not be determined as the boundary layer was seen to be separated.

With the increase in shock strength, the calculated total deflection of the streamlines ($\Delta_s+\varepsilon$) is now closer to the curve of the inclination of shock wave to undisturbed stream $\zeta$.

The calculated maximum external flow deflection through shock at the "interaction front" $\Delta_{s,max}$ is 9.2°.

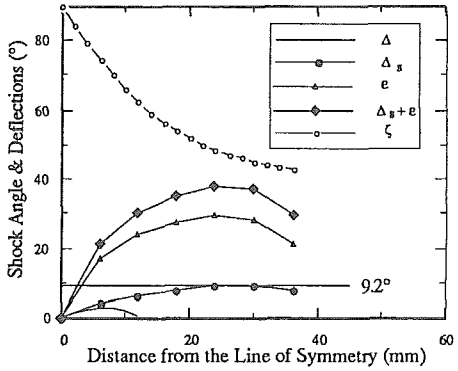


Fig. 20 Lateral Shock Wave Angles and Deflections, 17°Half-Cone, Re/m 58 million

Figure 21 shows all the same data for a 19° half-cone. The curve of the calculated total deflection of the streamlines ($\Delta_s+\varepsilon$) has now crossed the curve of the inclination of shock wave to undisturbed stream $\zeta$, indicating separation according to the model based on McCabe's criterion.

This corresponds to a maximum angle of the external flow deflection through shock at the "interaction front" $\Delta_{s,max}$ of 11.8°. This may be compared to the $\Delta_{s,max}$ of 9.2° from the 17° half-cone which its oil flow pattern indicates the beginning of boundary layer separation.

McCabe had a wedge completely spanned across the wind tunnel test section. His Theory predicts separation for Mach numbers of 1.96 and 2.94, which occur when the external flow deflections are 11.2° and 7.2°, respectively. These values may be compared to his experimental results which were 8.5° and 5.5°.

McCabe's results show that for Mach number of 1.96, the theoretical angle is 31.8% greater than the experimental angle while the present results for Mach number of 2.0 show that the predicted angle is 28.3% greater than the experimental angle. Therefore the discrepancy between the calculated and the observed values are of the same order as those of McCabe.

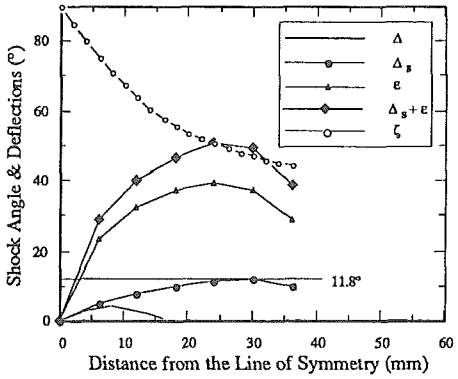


Fig. 21 Lateral Shock Wave Angles and Deflections, 19°Half-Cone, Re/m 58 million

## VII Comparison of Full and Half Cone Results

Figure 22 shows the maximum pressure ratios for both the 14° full and half cones. They are fairly close to each other, and they decrease gradually from the line of symmetry. However, the experimental maximum pressure ratios rise towards the ends, where the wall effects start becoming significant.

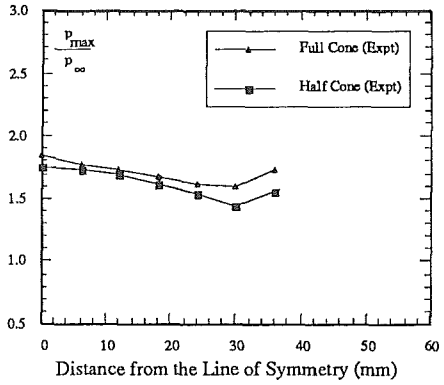


Fig. 22 Pressure Ratios, 14°Cone, Re/m 58 million

Similarly, Figure 23 shows the ratios for 20° cones and the results are similar, however, we note the differences are some what greater away from the line of symmetry showing that the wall effects are greater.

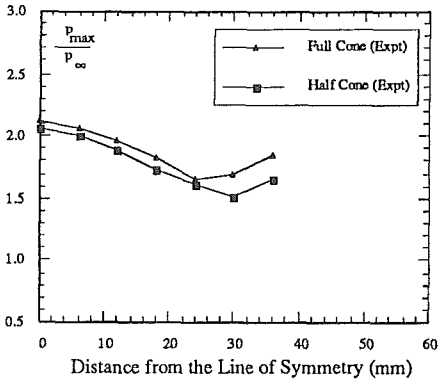


Fig. 23 Pressure Ratios, 20°Cone, Re/m 58 million

## VIII. Conclusions

The experiments have shown that the interaction of an incident conical shock wave with the turbulent boundary layer on a flat plate is of three-dimensional nature. In a $M_\infty = 2$ flow the boundary layer starts to separate with the shock generated by a 17° half-cone.

The surface pressure distributions show that there is a strong pressure gradient in the spanwise direction. There was no clear indication of a surface pressure plateau which is often used to imply the existence of streamwise separation.

There is a very small difference in the maximum pressure ratios obtained from the full and half cones.

A model for prediction of external flow conditions after the shock has been proposed. It is able to predict streamline deflections in the external flow and the boundary layer up to the point of separation.

## References


1. McCabe, A., The three-dimensional interaction of a shock wave with a turbulent boundary layer. The Aeronautical Quarterly, 231-252, August 1966.

2. Stollery, J. L., Glancing shock-boundary layer interactions. AGARD-FDP-VKI, Special Course on Three-Dimensional Supersonic and Hypersonic Flows Including Separation, England, 1989.

3. Migotsky, E. and Morkovin, M. V., Three-dimensional shock-wave reflections. Aeronautical Science, 484-489 & 504, July 1950.

4. Panov, Yu. U. , Interaction of incident three-dimensional shock with a turbulent boundary layer. Mekhanika Zhidkosti I Gaza Vol 3 No 3, 158-161, 1968.

5. Kussoy, M. I, Viegas, J. R. and Horstman, C. Investigation of a three-dimensional shock wave separated turbulent boundary layer. The Aeronautical Quarterly, Vol 18 No 2, 1477-1484, 1980.

6. Moeckel, W. E. and Connors, J. F., Charts for the determination of supersonic air flow against inclined planes and axially symmetric cones. NACA Technical Note No 1373, July 1947.

7. Crabtree, L. F., Kuchemann and D., Sowerby, L., Three-dimensional boundary layers. Laminar Boundary Layers, Fluid Motion Memoirs, Oxford University Press, 488-491, 1963.

8. Liepmann, H. W. and Roshko, A., Elements of gasdynamics. John Wiley & Sons, 1965.

9. Bogdonoff, S. M.,Three-dimensional shock wave/turbulent boundary layer interactions: Some observations and conjectures. Three-Dimensional turbulent Boundary Layer Symposium, IUTAP, 233-241, Berlin, 1982.

10. Delery, Jean M., Shock wave/turbulent boundary layer interaction and control. Progress in Aerospace Science, Vol 22, 209-280, 1985.

11. Bogdonoff, S. M.,Observation of three-dimensional "Separation" in shock wave turbulent boundary layer interactions Three-Dimensional turbulent Boundary Layer Symposium, IUTAP, 37-55, London, 1986.